PHYSICAL REVIEW C VOLUME 9, NUMBER 1 JANUARY 1974

# Symmetric fission in the neutron-induced fission of $^{255}$Fm†

R. C. Ragaini, E. K. Hulet, R. W. Lougheed, and J. Wild
*Lawrence Livermore Laboratory, University of California, Livermore, California 94550*
(Received 9 July 1974)

The kinetic energy distributions of coincident fission fragments from the thermal-neutron-induced fission of $^{255}$Fm and $^{251}$Cf have been measured with phosphorus-diffused silicon detectors. The most probable values for the postneutron total kinetic energy are $192.5 \pm 2.9$ MeV for $^{255}$Fm and $182.1 \pm 2.7$ MeV for $^{251}$Cf. Fragment mass distributions were calculated without applying neutron emission corrections. The resultant mass and kinetic energy distributions for $^{255}$Fm indicate a predominantly asymmetric mass division combined with appreciable symmetric fission. Fragment pairs near mass symmetry were found to be unusually energetic, which is a characteristic shared with symmetric fission in $^{257}$Fm and $^{258}$Fm. These results are well described by the two-center model of fission. Thermal-neutron-induced fission cross sections were measured as $3400 \pm 170$ b for $^{255}$Fm and $4800 \pm 250$ b for $^{251}$Cf.

[NUCLEAR REACTIONS, FISSION $^{255}$Fm$(n,f)$, $^{251}$Cf$(n,f)$, $E = 0.025$ eV; measured $\sigma$, fragment $E$; deduced fragment masses.]

## I. INTRODUCTION

Recent experiments measuring the kinetic energies of fragments produced by the spontaneous fission[1,2] (SF) and the thermal-neutron-induced fission[1] $(n,f)$ of $^{257}$Fm have shown that in the transition from $^{257}$Fm to $^{258}$Fm the primarily asymmetric mass distribution becomes predominantly symmetric. However, a recent radiochemical study[3] of $^{256}$Fm(SF) has shown its mass distribution to be largely asymmetric, with a peak-to-valley ratio of approximately 12. We have studied prompt fission following neutron absorption by $^{255}$Fm in order to evaluate the effect of excitation energy in this region, where there is a rapid transition from asymmetric to symmetric mass yields, and to compare our results with theoretical predictions.

Fission theory has provided several alternative explanations for the asymmetric mass distribution in fission. In one qualitative explanation, asymmetry is explained by strong shell effect within the residual fission product nuclei.[4] Other explanations, offering much more detail, have resulted from mapping the potential energy surface with the degree and the symmetry of nuclear deformation. Calculations with different static models have been carried out to deformations either just beyond the second or outer barrier[5-12] using a single potential, or, by using two-center potentials,[13-20] to the point of scission. Either treatment leads to the same qualitative conclusion—that asymmetric fission is fairly well localized in the actinide region and that there are transitions to symmetric fission just below $^{228}$Ra and just above $^{258}$Fm. Although the same conclusion has been reached from both the single- and the two-center potential models, the physical reasons for reaching this conclusion are quite different. Because of this, a choice of theoretical models is opened to experimental test by studying the mass and kinetic energy distributions from the prompt fission of $^{256}$Fm*.

Calculations made by Möller and Nilsson[5,9] using a liquid-drop model corrected for single-particle effects show that the minimum energy path for fission is always through a symmetric inner barrier and through an outer barrier that is asymmetric or symmetric, depending on the nuclide $(Z,A)$. Saddle points for both asymmetric and symmetric distortions are available at the outer barrier, and the one lying lower in energy would presumably govern the mass split at the scission point. For the heavier actinides the outer barrier is only a few MeV above the ground state, and asymmetric distortions are favored over symmetric ones by only a few tenths of an MeV. Thus, at excitation energies well above the level of the outer barrier, the effects of this barrier on the mass split should not be seen; a predominance of symmetric fission, which is prescribed by the inner barrier, would be seen. Basing their predictions on their calculations of the outer barrier heights, Tsang and Wilhelmy[21] suggested that $^{256}$Fm* should fission symmetrically.

The two-center model developed by Mosel and co-workers[13-18] allows calculation of the potential energy surfaces to much greater deformations than the single-potential model of Strutinski and Nilsson. As a result, it is possible to describe the energy surface from the ground state of the fissioning nucleus to the configuration of two completely separated fragment nuclei. From such calculations, it was concluded that shell structure in nascent *fragments* is important in the very early stages of the fission process, particularly in the descent from the outer saddle to the scission point.[14] The effect of fragment shells becomes especially important in determining the mass split when both fragments are doubly magic $^{132}$Sn nuclei, such as might occur in the fission of $^{264}$Fm. Thus, the transition from asymmetric fission in the light fermium isotopes to symmetric fission in the heavier ones is due to the fragments approaching closed proton and neutron shells ($Z=50$, $N=82$).[17] If this explanation should be correct, then excitation energy from binding a neutron should not be the primary cause of symmetric fission in the heavy fermium isotopes. Based on this model, we would not expect a dramatic increase of symmetric fission for $^{255}$Fm-$(n,f)$ compared to $^{256}$Fm(SF). Rather, some broadening of the mass distribution might be expected due to slight washing out of shell structure at ~6.5 MeV excitation energy in $^{256}$Fm*.

## II. EXPERIMENTAL

Isotopically pure samples of 20.3-h $^{255}$Fm were prepared by chemically separating it from its parent, 40.6-day $^{255}$Es. The $^{255}$Es was produced in 0.035% abundance, relative to $^{253}$Es, by neutron irradiation of lighter actinides in the high flux isotope reactor at the Oak Ridge National Laboratory. A few hours before each fission experiment the $^{255}$Fm, in equilibrium with $^{255}$Es, was separated from ~2.1 $\mu$g of Es (mainly $^{253}$Es) by elution from a cation exchange column with $\alpha$-hydroxyisobutyric acid. Einsteinium and californium were reduced to undetectable amounts by repeating this ion-exhange separation once. Common elements that would contribute to the mass of the final sample were separated in a small quartz column contining Dowex 50×12 colloidal resin. After adsorption from 0.5 *M* HCl, the fermium was carefully eluted with 2 and 6 *M* ultrapure HCl. The final target for fission counting was then prepared by electroplating the $^{255}$Fm from 0.001 *M* $HNO_3$ to form a 2-mm-diam spot on a ~175-$\mu$g/cm$^2$ gold foil. We required approximately 4 h to separate and prepare the $^{255}$Fm target chemically, place it in the counter, and then bring the reactor to full power before starting the first fission count.

Three $^{255}$Fm samples were prepared and fission counted, but only the data collected from the third and final run are reported here. This target contained $(3.37\pm0.10)\times10^{10}$ atoms of $^{255}$Fm as determined by $\alpha$-counting and $\alpha$-pulse analyses. No activities other than $^{251}$Cf ($\alpha$ daughter of $^{255}$Fm) were detected in the sample after complete decay of the $^{255}$Fm. As a gauge of source thickness, we measured the resolution of $^{251}$Cf $\alpha$ particles, and these were found to be about 35 keV full width at half maximum (FWHM).

In addition to the $^{255}$Fm target, a spontaneous-fission source of $^{252}$Cf and a neutron flux monitor of $^{233}$U were prepared on 180- and 230-$\mu$g/cm$^2$ gold foils, respectively. The isotopically pure $^{233}$U (separated from $^{237}$Np) was used as a reference standard for measuring the thermal-neutron-fission cross sections of $^{255}$Fm and its $\alpha$ daughter, $^{251}$Cf. This standard contained $1.334\pm0.007$ ng of $^{233}$U, a value determined by $\alpha$ counting.

The $^{255}$Fm target was mounted onto a four-position target wheel located between two phosphorus-diffused silicon detectors covered with aluminum collimators to restrict the entry angle to 50°. The other targets on the wheel consisted of the electroplated $^{252}$Cf source for energy calibration, the $^{233}$U source, and a blank ~175-$\mu$g/cm$^2$ gold foil for background runs. All sources were sandwiched between the gold backing and the ~175-$\mu$g/cm$^2$ gold cover foils in order to prevent detector contamination. The source-to-detector distance was approximately 2 mm. The assembly, along with an aluminum-covered noise detector, was mounted inside an evacuated aluminum chamber and inserted into the Livermore pool-type reactor thermal column in a thermal flux of $2\times10^{11}$ $n$/cm$^2$ sec with a cadmium ratio for gold of 600. The detectors were cooled to −25°C by circulating refrigerated alcohol through cooling lines attached to the detector mounting plates. The target turning shaft, cooling lines, and detector leads were carried outside the thermal column through a 2-m-long evacuated tube. Fast linear electronics were used to process the coincident fragment pulses for pulse-height analysis. Pulse pile-up rejection was employed, and noise pickup was eliminated by the use of the noise detector in an anticoincidence mode. Upon insertion into the $2\times10^{11}$ $n$/cm$^2$ sec flux, the leakage currents of the cooled detectors immediately rose from less than 1 $\mu$A to 12 $\mu$A at 200-V reverse bias and remained there until the end of the experiment.

The amplified pulses were fed to a two-parameter pulse-height analyzer operating in a 512-event buffer mode. The pulse heights of the coincident fragments were buffered onto magnetic tape for subsequent computer sorting and analysis. Details of the experimental procedure have been published previously.[22]

The coincident fission-fragment counting rate from the $^{255}$Fm-$^{251}$Cf target increased from 500 counts/min at the beginning of the experiment to 660 counts/min at the end. Fission counts from $^{256}$Fm(SF) (produced by $n,\gamma$ reactions) were less than 1% of the prompt fissions from $^{255}$Fm$(n,f)$, since the neutron-capture cross section of $^{255}$Fm is only 30 b.[23]

The experiment was carried out for seven days in order to follow the decay of $^{255}$Fm to $^{251}$Cf. Approximately 15 fission spectra were taken over the course of the experiment. For calibration and flux monitoring purposes, the fission spectra of $^{255}$Fm and $^{251}$Cf were interspersed with fission spectra from the $^{252}$Cf and $^{233}$U targets. At the midpoint of the first fission spectrum taken, the source was 80.0% $^{255}$Fm and 20.0% $^{251}$Cf. At the midpoint of the last spectrum taken, the target was 99.7% $^{251}$Cf.

The fission cross section of $^{251}$Cf was determined from the fission rate during the last few spectra, when the sample was essentially pure $^{251}$Cf. A cross section of 4800± 250 b was calculated for $^{251}$Cf from the ratio of the fission rate of $^{251}$Cf to that of the $^{233}$U standard, the measured atom ratios in each, and the known thermal-neutron-fission cross section[24] of 531 b for $^{233}$U. A thermal-neutron-fission cross section of 3400± 170 b was calculated for $^{255}$Fm in a similar way, but the fission rate was determined by least-mean-squares fitting of the growth-decay curve of the gross fission rates. In the fitting, which included 14 decay points taken over 7 days, gross fission rates were normalized to a constant neutron flux by using the fission rate of the $^{233}$U standard. The half-lives of $^{251}$Cf (898 yr) and $^{255}$Fm (20.3 h) were held as fixed parameters. A standard deviation of 3.7% was obtained in this least-mean-squares fit.

Energy calibrations were based on an average post neutron emission energy of 183.9 MeV for $^{252}$Cf, which is an average of the results of Schmitt, Neiler, and Walter[25] and Whetstone.[26] A correction was made for the pulse-height defect according to the method of Schmitt, Kiker, and Williams.[27] Care was taken to operate the detectors in the saturation region to ensure the validity of the calibration procedure. In order to include the effects of energy losses in the gold foil and the detector window, the $^{252}$Cf fragments were analyzed under the identical conditions as were the $^{255}$Fm and $^{251}$Cf fragments. The calibration constants thus obtained included the corrections for energy losses. These calibration constants were then used to analyze the energy spectrum of the $^{255}$Fm and $^{251}$Cf fragments.

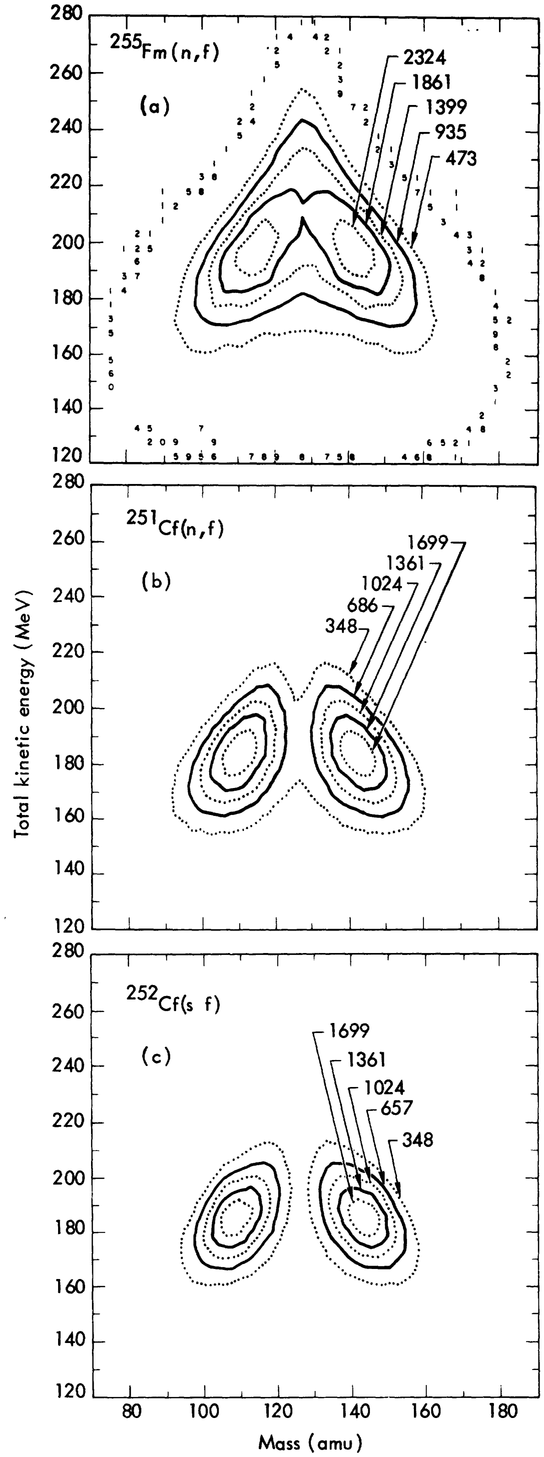


FIG. 1. Contour diagrams of counts vs provisional fragment mass and postneutron total kinetic energy: (a) $^{255}$Fm$(n,f)$ for 172 881 events are grouped into 5.0-MeV and 3.4-amu bins; (b) $^{251}$Cf$(n,f)$ for 367 114 events are grouped into 2.5-MeV and 1.7-amu bins; $^{252}$Cf(SF) for 332 434 events are grouped into 2.5-MeV and 1.7-amu bins.

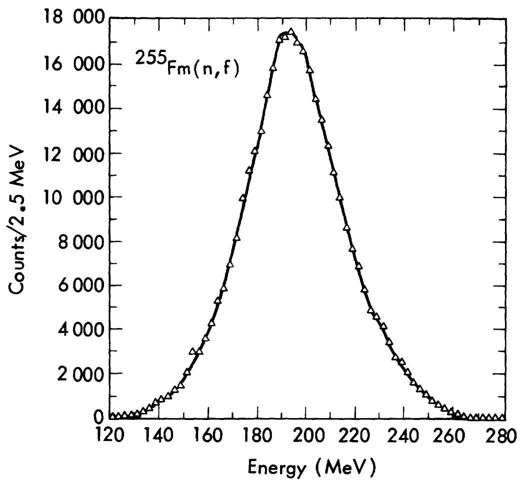


FIG. 2. Postneutron emission total kinetic energy distribution for the thermal-neutron-induced fission of $^{255}$Fm. The most probable kinetic energy is 192.5 ± 2.9 MeV. The FWHM is 42.5 MeV.

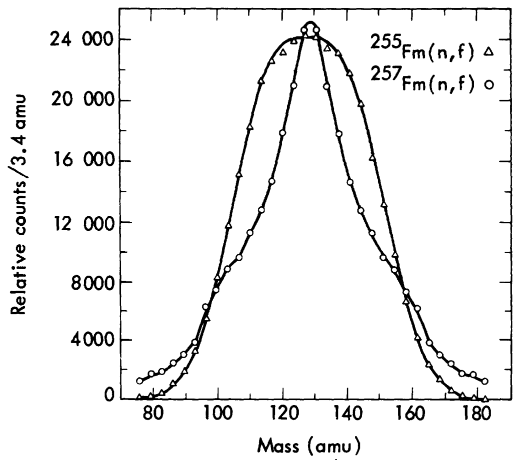


FIG. 3. Provisional mass distributions for the thermal-neutron-induced fission of $^{255}$Fm and of $^{257}$Fm. The $^{257}$Fm distribution is taken from Ref. 1 and represents 15 900 fissions.

No corrections were made for neutron emission since Balagna *et al.*[2] had shown that the mass distribution is extremely sensitive to $\nu(M)$. Their use of a $\nu(M)$ correction corresponding to the $^{252}$Cf $\nu(M)$ created a double-humped preneutron emission mass-yield curve for $^{251}$Fm(SF) with a peak-to-valley ratio of 1.5, whereas a constant $\nu(M)$ value of 2 created a flat-topped curve with no valley.[2] Therefore, in order not to distort the data in any arbitrary way, we present the mass data which correspond to the provisional masses of Schmitt, Neiler, and Walter.[25] No corrections were made for instrumental resolution.

## III. RESULTS

Figure 1(a) shows the results for thermal-neutron fission $^{255}$Fm represented as a contour diagram of counts vs fragment mass and total kinetic energy. This plot was obtained by subtracting out the events from the thermal-neutron fission of $^{251}$Cf, which was done by weighting the $^{251}$Cf fission spectra according to the amount of $^{251}$Cf in the target and using the fission cross sections for $^{255}$Fm and $^{251}$Cf derived from fission rates as a function of time. This procedure amounted to a subtraction of 141 045 $^{251}$Cf fission events out of a total of 313 926 gross fission events, a 45% correction. The highest points (2787 events) occur at the asymmetric fission masses of 114 and 142 for a postneutron emission energy of 194 MeV. The most energetic contour on the plot occurs at mass 128 and equals 254 MeV (473 events out of a total of 172 881 events). Figure 2 shows a plot of the kinetic energy for $^{255}$Fm$(n,f)$ obtained by summing over all fragment masses. The average postneutron kinetic energy is computed $[\langle E\rangle = \sum_i N_i(E_i)E_i/N]$ to be 192.5 ± 2.9 MeV.

In Fig. 3, we show the mass distribution from $^{255}$Fm$(n,f)$ without neutron correction, a relatively flat distribution. A neutron correction $\nu(M)$ similar to that for $^{252}$Cf(SF), in which there is a sharp drop in $\nu(M)$ at symmetric fission, would produce a dip at mass symmetry in the calculated preneutron-emission mass yields. Since a detailed behavior of $\nu(M,E)$ is not known for the fermium isotopes, it was felt that the provisional mass distribution for $^{255}$Fm$(n,f)$ would be the most valid method of presenting the data.

Figure 1(b) represents the counts vs mass and energy for $^{251}$Cf. This contour diagram is very similar to the analogous plot for $^{252}$Cf(SF) shown

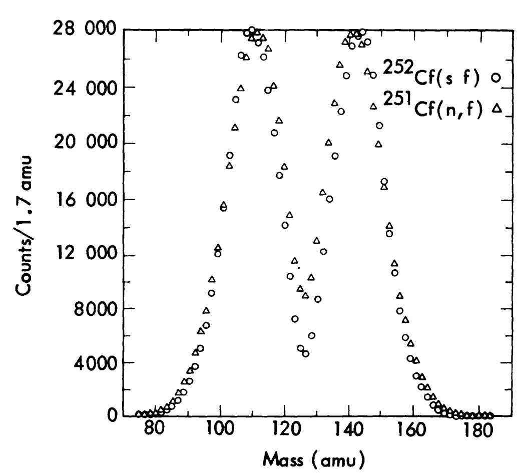


FIG. 4. Provisional mass distributions for the thermal-neutron-induced fission of $^{251}$Cf and for the spontaneous fission of $^{252}$Cf.

in Fig. 1(c), except that there are more events in the region near a symmetric mass split. Figure 4 shows the mass distribution for $^{251}$Cf($n,f$), which again resembles the $^{252}$Cf(SF) mass distribution. The peak-to-valley ratios are 3.1 for $^{251}$Cf($n,f$) and 5.3 for $^{252}$Cf(SF). The FWHM for the $^{251}$Cf-($n,f$) kinetic curve was 36.5 MeV, compared to 31.7 MeV for the $^{252}$Cf (SF) energy curve. The exact difference in target thicknesses is unknown, and therefore the effect of this difference on the mass distribution is not known. The average post-neutron total kinetic energy for $^{251}$Cf thermal-neutron-induced fission was computed to be $182.1 \pm 2.7$ MeV.

Table I compares our kinetic energy measurements to those for other fermium and californium isotopes. Our reported errors of ±2.9 and ±2.7 MeV for $^{255}$Fm and $^{251}$Cf, respectively, include a $2\sigma$ value (1.0 MeV) for the variation of the different runs about the mean energies reported. The errors also include an estimate to account for any differences in thickness between the combined $^{255}$Fm-$^{251}$Cf target and the $^{252}$Cf target. In general, the results seem quite reasonable for the californium isotopes, considering the errors quoted for the measurements. The $^{255}$Fm($n,f$) and $^{257}$Fm(SF) data agree quite well; however, the $^{257}$Fm($n,f$) $\langle E\rangle$ value appears too low. Balagna *et al.*[2] have measured the average energy for $^{257}$Fm(SF) to be $195.1 \pm 2.9$ MeV, whereas John *et al.*[1] measured the average postneutron energy for $^{257}$Fm($n,f$) to equal 180 MeV. This may have been the result of inadequate statistics. The approximate total preneutron kinetic energy of 195 MeV for $^{255}$Fm ($n,f$) is higher than the value of 191 MeV calculated from Viola's[30] empirical relationship $\langle E\rangle = 0.1071\, Z^2/A^{1/3} + 22.2$, based on the liquid-drop model. This disagreement is understandable considering that 12% of the events have energies above 220 MeV. Since the predicted energies decrease as $A$ increases, the preneutron kinetic energy (198 MeV) reported[2] for $^{257}$Fm(SF) is in greater disagreement with the empirical curve (190 MeV) than the $^{255}$Fm($n,f$) energy. It should be pointed out that Viola's relationship was intended to predict the trend for asymmetric fission and did not anticipate the symmetric fission which occurs in $^{255}$Fm($n,f$) and $^{257}$Fm(SF).

Since fragments coming from symmetric fission have higher kinetic energies than those associated with asymmetric fission, we can differentiate symmetric fission by the unusually high total energies of these events. Figure 5 illustrates the changes in mass distribution as the total kinetic energy of fission increases. The double-humped distribution gradually shifts over to a single-humped curve which becomes narrower as the kinetic energy rises. A single-humped distribution first occurs at 220–225 MeV, and we have assumed that all events at or above this energy

TABLE I. Average postneutron total kinetic energies.

| | $\langle E\rangle$ (MeV) | FWHM (MeV) | Ref. |
|---|---|---|---|
| $^{254}$Fm (SF) | 186 ±2 | 27.6 | 28 |
| $^{255}$Fm ($n,f$) | 192.5±2.9 | 42.5 | This work |
| $^{257}$Fm (SF) | 195.1±2.9 | 36.4 | 2 |
| $^{257}$Fm ($n,f$) | 180 | | 1 |
| $^{250}$Cf (SF) | 181.8±2.7 | 30.2 | 29 |
| $^{251}$Cf ($n,f$) | 182.1±2.7 | 36.5 | This work |
| $^{252}$Cf (SF) | 184.1±2.8 | 30.8 | 29 |
| $^{254}$Cf (SF) | 181.8±2.7 | 33.8 | 29 |

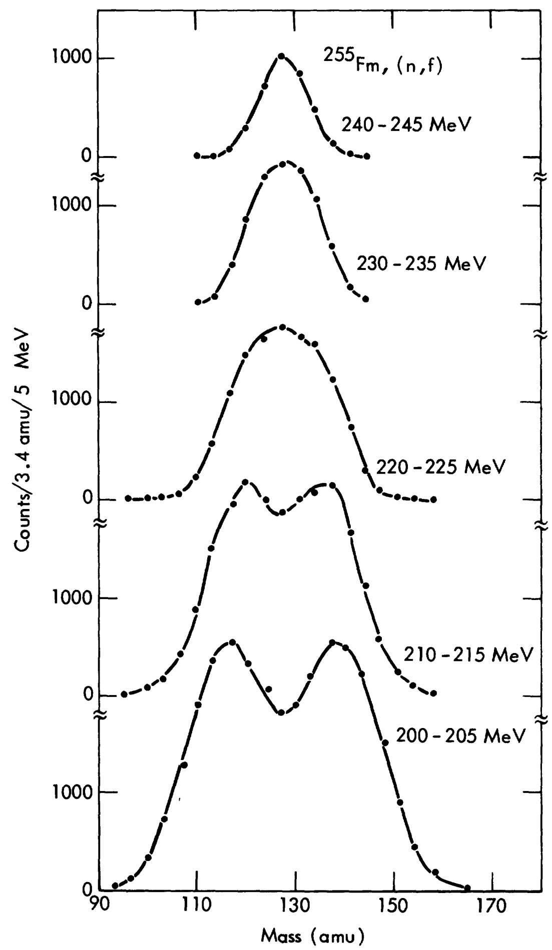


FIG. 5. Provisional mass distributions for $^{256}$Fm* fission grouped as a function of their total kinetic energies. Each curve shows the mass distribution at a fixed-total kinetic energy (within a 5-MeV band). They are constant energy cuts across the mass-energy contours of Fig. 1(a).

originated from symmetric fissions. Inasmuch as we have no way of distinguishing symmetric events below this energy, our cutoff at 220 MeV is merely qualitative and has been used arbitrarily in estimating the percentage of symmetric fission. Approximately 12% of the events have kinetic energies greater than 220 MeV. From the relative portion of such events, we describe the mass distribution from $^{256}$Fm* fission as primarily asymmetric with an appreciable symmetric component. We believe this method of estimating symmetry offers a higher sensitivity than total peak-to-valley ratios obtained from radiochemical measurements, since for the heavier fermium isotopes, a valley is barely discernible, if it appears at all. Until the valley is fully filled, the conclusions from radiochemical peak-to-valley ratios will likely be quite different from the conclusions reached from coincident-fragment energy measurements. Keeping these limitations in mind, we compare only those features in the fission of $^{256}$Fm* that are common to both types of measurements, namely the mass-yield curves.

Using radiochemical techniques, Flynn and coworkers[3] have shown the mass-yield curve from $^{256}$Fm(SF) to have a peak-to-valley ratio of 12. We observe no valley in our provisional mass distribution (Fig.3); therefore, it seems evident that there is more symmetric mass division from the fission of $^{256}$Fm* than from the spontaneous fission of $^{256}$Fm. This increase in near-symmetric mass division with an increase in excitation energy is consistent with the behavior of the lighter actinides. Flynn *et al.*[31] used radiochemical methods to determine a peak-to-valley ratio of 2.5 for $^{255}$Fm-$(n,f)$. Our data are consistent with their radiochemical results after taking into account the broadening due to the resolution of the silicon detectors and the broadening from neutron emission.

## IV. DISCUSSION

The most notable feature of our $^{256}$Fm* fission results is the unusually high fragment energies associated with masses near symmetric division This is seen by comparing Fig. 1(a) with Figs. 1(b) and 1(c). This same high-energy component is also characteristic of symmetric fission in $^{257}$Fm and $^{258}$Fm*. These distinctive symmetric events predominate in the fission of $^{258}$Fm*. Since the mass-energy contours shown in Fig. 1(c) are remarkably similar to those for $^{257}$Fm(SF), we have concluded that the neutron-induced fission of $^{255}$Fm gives mass and energy distributions equivalent to the spontaneous fission of $^{257}$Fm.

High kinetic energies from fragments near mass symmetry have now been observed in the neutron-induced fission of $^{255}$Fm and $^{257}$Fm and the spontaneous fission of $^{257}$Fm, but not in the fission of lighter actinides. As noted in earlier reports,[1,2] this is obviously related to the low internal excitation energy of the fragments caused by their spherical rigidity upon approaching the magic nucleon numbers $Z=50$, $N=82$. The total kinetic energy of fragments from some events approximates the $Q$ value of the reaction, indicating nearly zero internal excitation energy. These properties of symmetric fission in the fermium isotopes are the inverse of those found in symmetric fission in $^{233}$U, $^{235}$U, and $^{239}$Pu. For the latter nuclides, there is a pronounced dip in the kinetic energy released for near-symmetric mass division and a corresponding increase in fragment excitation energy (an increase in $\nu$).[32] Fission products from near-symmetric division of these nuclei lie in a region that is softer toward deformation than products from the near-symmetric fission of the fermium isotopes. Thus, the contrasting behavior in the division of kinetic and excitation energy by the lighter and heavier actinides is apparently related to the softness of the fragments toward deformation. We infer from such correlations that the partitioning of energy *and* mass in the fission process is governed by fragment shell structures.

We discern two modes of fission (asymmetric and symmetric) from Fig. 1(a), since symmetric fission —as a separate, observable mode—is distinguishable by having unusually high fragment energies. From this contour plot and also from the ones for $^{257}$Fm(SF) and $^{257}$Fm$(n,f)$,[1] a new type of symmetric division appears superimposed upon a normal asymmetric one. This suggests a genuine form of symmetric fission arising only from symmetric deformations. The mass and energy distributions from the asymmetric mode of fissioning in these isotopes seem about as expected for nuclei in this mass range. In this mode, near-symmetric masses come from symmetric scission of asymmetrically deformed nuclei. In this respect a distinction is made between a symmetric mass division and genuine symmetric fission.

Our conclusion regarding the appearance of two distinct fission modes suggests a relationship to the two-mode fission hypothesis first proposed by Turkevitch and Niday.[33] This hypothesis has been used to interpret mass distributions from fission of excited nuclei in the Ra-Ac region where the relative probabilities for symmetric and asymmetric fission are about equal at excitation energies near 20 MeV. A three-peaked mass distribution representing symmetric and asymmetric fission modes has also been observed in the helium-ion-induced fission of $^{233}$U and the fission of $^{232}$Th caused by reactor spectrum neutrons.[34] Most importantly, there was an increasing yield of the symmetric mode with increasing excitation energy. Therefore, a possibility exists that the symmetric component that we find in the neutron fission of $^{255}$Fm and $^{257}$Fm is a result of excitation energy. An enhancement of symmetric division caused by excitation from the neutron separation energy is very evident from the two radiochemical studies of $^{256}$Fm fission, but this increase of valley-to-peak ratios with excitation energy seems similar to the general trend established for the lighter actinides and for the prompt fission of $^{252}$Cf* reported here. Thus, this customary increase of the symmetric mode with rising excitation energy appears unrelated to the *onset* of the new type of symmetric fission in the heavy fermium isotopes. Our conclusion here is also based on the large increase in symmetric fission for $^{257}$Fm-$(n,f)$ compared to $^{255}$Fm$(n,f)$ in which the excitation energies of each of these nuclides before fissioning are comparable. At the moment, we view this symmetric mode as a direct consequence of strong shell effects in fragment nuclei near doubly closed-shell $^{132}$Sn.

The mass and kinetic energy distributions from the fission of $^{256}$Fm* are in good agreement with the qualitative predictions of the two-center model of fission. Results from calculations using this model correctly anticipated a transition from asymmetric fission in the light fermium isotopes to symmetric fission in the heavier ones[17] and an increase in the total kinetic energy of fragments near mass symmetry, together with a decrease in internal excitation energy.[16] A quantitative comparison is available from the total kinetic energy of the fragments. Assuming a symmetric division of charge and mass from the fission of $^{256}$Fm, Schmitt and Mosel[16] calculate a total kinetic energy of ~210 MeV, while we obtained 212 MeV for $\overline{E}_k$ $(A = 128)$.

On the other hand, our results disagree somewhat with the prediction of Tsang and Wilhelmy[21] that $^{256}$Fm* should fission primarily symmetrically.[35] Their prediction was based largely upon the relation of the excitation energy to the height of the second or outer barrier. In the case of $^{256}$Fm*, asymmetric deformations at this barrier are favored over symmetric ones by a saddle ~0.2 MeV lower in energy. However, Tsang and Wilhelmy expected the excitation energy after neutron capture to be ~3.2 MeV greater than the outer barrier, leading them to propose that symmetric distortions should be preferred equally to asymmetric ones. This theory excludes completely the effects of fragment shells upon the mass division and depends instead on potential energy surfaces originating from shell structure of the parent fissioning nucleus. Since the mass division of $^{256}$Fm* fission is primarily asymmetric and, therefore, since their model failed this test, we feel the influence of fragment shells needs to be included in a suitable theory.

Wilkins and Steinberg,[36] in extending earlier approaches,[37-40] have incorporated the effect of fragment shells on the total potential energy of the system when at large deformations. In this model, potential energies for strongly deformed fragments were calculated for the case where the fragments were still joined (somewhere between the outer saddle and scission points). Fragment pairs yielding the lowest total potential energy were assumed to determine the most probable mass and charge distributions. With this simplified model, the mass distributions of many nuclides were surprisingly well fitted, particularly by slightly adjusting the deformation parameter $\beta$ of the fissioning nucleus where the mass division is decided.

An asymmetric mass distribution for the thermal-neutron-induced fission of $^{255}$Fm was anticipated by Wilkins and Steinberg.[36] However, contrary to our results, they estimated that the total kinetic energy released in symmetric division would be a nominal 200 MeV rather than the unusually high energies observed. To account for this discrepancy, it would have been necessary for them to let some portion of the mass divisions be determined at a much smaller $\beta$, such as that $\beta$ associated with the inner symmetric barrier. Further refinements of this model may allow this to be done, but at this time it appears to have some arbitrary features.

All of the theoretical approaches that we have compared with our experimental data are limited to the extent that they are unable to fully reproduce the details given in the contour plot of Fig. 1(a). We note that these approaches are rooted in a common base, namely, the calculating of quasistatic potential energy surfaces for nuclei at very large deformations. Since static calculations are inherently limited in a dynamic process, further advancements in providing a detailed explanation of fission will eventually require a full dynamic treatment for deformations from the ground state to the scission point.

## ACKNOWLEDGMENTS

We take pleasure in acknowledging the helpful suggestions made by W. J. Swiatecki and C. F. Tsang. The computer codes were written by Robert Dickinson, who was invaluable in analyzing the data. We thank the operations and support staff of the Livermore pool-type reactor for their help, without whom the experiments could not have been carried out. We also thank the Division of Research of the U. S. Atomic Energy Commission and the Oak Ridge National Laboratory for the production and isolation of the einsteinium used in our experiments. The support and encouragement of Dr. W. E. Nervik of the Radiochemistry Division of the Lawrence Livermore Laboratory are acknowledged.

---

†Work performed under the auspices of the U. S. Atomic Energy Commission.


[1]W. John, E. K. Hulet, R. W. Lougheed, and J. J. Wesolowski, Phys. Rev. Lett. 27, 45 (1971).

[2]J. P. Balagna, G. P. Ford, D. C. Hoffman, and J. D. Knight, Phys. Rev. Lett. 26, 145 (1971).

[3]K. F. Flynn, E. P. Horwitz, C. A. A. Bloomquist, R. F. Barnes, R. K. Sjoblom, P. R. Fields, and L. E. Glendenin, Phys. Rev. C 5, 1725 (1972).

[4]P. Fong, Phys. Rev. 102, 434 (1956).

[5]P. Möller and S. G. Nilsson, Phys. Lett. 31B, 283 (1970).

[6]H. C. Pauli, T. Ledergerber, and M. Brack, Phys. Lett. 34B, 264 (1971).

[7]C. Gustafsson, P. Möller, and S. G. Nilsson, Phys. Lett. 34B, 349 (1971).

[8]H. Schultheis and R. Schulteis, Phys. Lett. 34B, 245 (1971).

[9]P. Möller, Nucl. Phys. A192, 529 (1972).

[10]V. V. Pashkevich, Nucl. Phys. A169, 275 (1971).

[11]J. R. Nix, Annu. Rev. Nucl. Sci. 22, 341 (1972).

[12]M. Bolsterli, E. O. Fiset, J. R. Nix, and J. L. Norton, Phys. Rev. C 5, 1050 (1972).

[13]D. Scharnweber, W. Greiner, and U. Mosel, Nucl. Phys. A164, 257 (1971).

[14]U. Mosel, J. Maruhn, and W. Greiner, Phys. Lett. 34B, 587 (1971).

[15]U. Mosel and H. W. Schmitt, Phys. Rev. C 4, 2185 (1971).

[16]H. W. Schmitt and U. Mosel, Nucl. Phys. A186, 1 (1972).

[17]M. G. Mustafa, U. Mosel, and H. W. Schmitt, Phys. Rev. Lett. 28, 1536 (1972).

[18]M. G. Mustafa, U. Mosel, and H. W. Schmitt, Phys. Rev. C 7, 1519 (1973).

[19]B. Slavov, J. E. Galonska, and A. Faessler, Phys. Lett. 37B, 483 (1971).

[20]G. D. Adeev, P. A. Cherdantsev, and I. A. Gamalya, Phys. Lett. 35B, 125 (1971).

[21]C. F. Tsang and J. B. Wilhelmy, Nucl. Phys. A184, 417 (1972).

[22]J. J. Wesolowski, W. John, and J. Held, Nucl. Instrum. Methods 83, 208 (1970).

[23]R. W. Hoff, J. E. Evans, E. K. Hulet, R. J. Dupzyk, and B. J. Qualheim, Nucl. Phys. A115, 225 (1968).

[24]Nucl. Data B6(No. 3), 275 (1971).

[25]H. W. Schmitt, J. H. Neiler, and F. J. Walter, Phys. Rev. 141, 1146 (1966).

[26]S. L. Whetstone, Jr., Phys. Rev. 131, 1232 (1963).

[27]H. W. Schmitt, W. E. Kiker, and C. W. Williams, Phys. Rev. 137, B837 (1965).

[28]R. Brandt, S. G. Thompson, R. C. Gatti, and L. Phillips, Phys. Rev. 131, 2617 (1963).

[29]D. C. Hoffman, G. P. Ford, and J. P. Balagna, Phys. Rev. C 7, 276 (1973).

[30]V. E. Viola, Jr., Nucl. Data A1, 391 (1966).

[31]K. F. Flynn, J. E. Gindler, R. K. Sjoblom, and L. E. Glendenin, in *Third International Symposium on the Physics and Chemistry of Fission, Rochester, N. Y., 13–17 August 1973* (International Atomic Energy Agency, Vienna, 1973), Paper 209 reported by J. P. Unik.

[32]E. K. Hyde, *The Nuclear Properties of the Heavy Elements* (Prentice Hall, Englewood Cliffs, N. J., 1964), Vol. III, p. 187.

[33]A. Turkevich and J. B. Niday, Phys. Rev. 84, 52 (1951).

[34]See Ref. 32, p. 330.

[35]C. F. Tsang and J. B. Wilhelmy's definition of "symmetric fission" is unclear. Although they have stated that $^{256}$Fm* should fission symmetrically, they have also equated this term to a mass distribution having a peak-to-valley ratio near 1. They also indicated that the mass distributions from the neutron-induced fission of $^{255}$Fm and $^{257}$Fm should be much alike, which they are not.

[36]B. D. Wilkins and E. P. Steinberg, Phys. Lett. 42B, 141 (1972).

[37]F. Dickmann and K. Dietrich, Nucl. Phys. A129, 241 (1969).

[38]H. W. Schmitt, in *Proceedings of the Second International Symposium on Physics and Chemistry of Fission, Vienna, Austria, 1969* (International Atomic Energy Agency, Vienna, 1969), p. 67.

[39]V. S. Ramamurthy and R. Ramanna, in *Proceedings of the Second International Symposium on Physics and Chemistry of Fission, Vienna, Austria, 1969* (see Ref. 38), p. 50.

[40]A. V. Ignatyuk, Yad. Fiz. 7, 1043 (1968) [transl.: Sov. J. Nucl. Phys. 7, 626 (1968)].